Nonlocal Microplane Model for Fracture, Damage, and Size Effect in Structures

By Zdeněk P. Bažant,[1] Fellow, ASCE, and Joško Ožbolt[2]

Abstract: A generalized microplane model, which was previously developed to describe tensile cracking and nonlinear triaxial response of brittle-plastic materials in compression and shear, is implemented in a finite element code. To limit localization instabilities due to strain softening and the consequent spurious mesh-sensitivity, the recently proposed concept of nonlocal continuum with local strain (nonlocal damage) is adopted and combined with the microplane model. An effective numerical algorithm permitting large loading steps is developed by applying the idea of exponential algorithms previously used for creep. Problems due to nonsymmetry of the tangential stiffness matrix are avoided by using the initial elastic stiffness matrix in the incremental force-displacement relations. Numerical results demonstrate that the microplane model, which previously has allowed an excellent description of the test data on nonlinear triaxial behavior of concrete as well as unidirectional and multidirectional crack or crack shear, is endowed (in its nonlocal generalization) with the capability of also modeling tensile fracture. The model yields the correct transitional size effect observed in concrete and agrees with the recently proposed size effect law. The formulation is applicable to brittle-plastic materials in general.

Introduction

At present there basically exist two kinds of material constitutive models: (1) The macroscopic tensorial models, in which the constitutive relation is formulated in terms of the macroscopic continuum stress and strain tensors and their invariants; and (2) the microscopic nontensorial models, in which the micromechanics of deformation is described by some suitably simplified model and the constitutive material properties are characterized by a relation between the stress and strain components (or forces and displacements) on the microlevel. The former is the classical approach, which has led to important advances in the modeling of concrete (e.g., Chen and Chen 1975; Bažant and Bhat 1976; Willam and Warnke 1974; Gerstle 1980, 1981; Dougill 1976; Bažant and Kim 1979; Ortiz 1985; Cedolin et al. 1983; Lin et al. 1987). However, the more realistic macroscopic constitutive models for concrete are rather complicated and very difficult to identify from test data, since they contain many material parameters, typically more than 15, while the agreement with test data is still less than satisfactory. Recent extensive efforts have not succeeded in overcoming these drawbacks, and it seems that the macroscopic approach has already yielded what it can and that further great efforts can only provide diminishing returns.

More promising seems to be the second kind of material models, which use micromechanics ideas and now basically exist in two versions: the random particle system modeling of the aggregate structure, which, unfortunately, poses forbidding demands on computer time, and the microplane model. The latter requires more computer time than even the most sophisticated macroscopic models, but, with the present computer capabilities, is manageable even for larger finite element programs. Compared to the macroscopic constitutive models, the microplane model trades computer time for conceptual simplicity. The model need not bother with tensorial invariance restrictions (which are automatically satisfied a posteriori), only with a few stress and strain components on planes of various orientations, called the microplanes. A simple, nontensorial relation between these components defines the constitutive properties. The macroscopic stress and strain tensors are related to the microplane stresses by a virtual work relation and by a static or kinematic constraint.

The basic idea of microplane models, from the work of Taylor (1938), was initially applied only to metal plasticity and went under the name "slip theory." Extensions to nonsoftening behavior of rocks and soils were made by Zienkiewicz and Pande (1977) and Pande and Xiong (1982). Some conceptual modifications were needed to make Taylor's idea applicable to strain-softening brittle behavior (Bažant 1984b; Bažant and Oh 1983, 1985; Bažant and Gambarova 1984) and most recently to strain-softening brittle-plastic behavior, typical of concrete (Bažant and Prat 1988). So far, this latest formulation provided the most complete material model for concrete under tensile and compressive triaxial stress states. Since the deformation on various planes in the microstructure could no longer be called "plastic slip," the more general term "microplane" was coined (Bažant 1984b).

The stress and deformation interactions in the microstructure are, in essence, of two kinds: (1) Interactions over a distance; and (2) interactions between orientations. The microplane models take into account only the latter. The former can be most simply taken into account by the concept of a nonlocal continuum (Kröner 1968; Eringen and Edelen 1972; cf. Bažant and Oh 1986), in which the strain at a point depends not only on the strain at the same point but on the entire strain field in a certain neighborhood of the point. The nonlocal concept has already been proven to be a useful cure for the problems of localization instabilities, which are endemic for local continuum models. Applications of the nonlocal concept, however, have so far been confined to the macroscopic tensorial constitutive model. The objective of the present paper is to marry this concept to the more powerful microplane approach, thus gaining a model that can handle in a rather realistic manner both fracture (or damage localization) and nonlinear triaxial deformations.

First, we need to describe precisely the form of the microplane model to be used. Then we develop its nonlocal generalization. In the process, we also formulate a new, effective algorithm (of the exponential type) for the analysis of loading steps.

Review of Microplane Model

Basic Hypotheses and Strain Components

Hypothesis I

The strains on any microplane are the resolved components of the macroscopic strain tensor ϵ_{ij}. This hypothesis, which represents a kinematic constraint, yields the relations [Fig. 1(*a*)]

[1]Walter P. Murphy Prof. of Civ. Engrg., Ctr. for Advanced Cement-Based Matls., Northwestern Univ., Evanston, IL 60208-3109.

[2]Visiting Scholar, Northwestern Univ., Assoc. Prof. on leave from Tech. Univ. of Zagreb, Zagreb, Yugoslavia; presently, Res. Engr., Technische Universität Stuttgart, W. Germany.

Note. Discussion open until April 1, 1991. To extend the closing date one month, a written request must be filed with the ASCE Manager of Journals. The manuscript for this paper was submitted for review and possible publication on October 31, 1989. This paper is part of the ***Journal of Engineering Mechanics***, Vol. 116, No. 11, November, 1990. ©ASCE, ISSN 0733-9399/90/0011-2485/$1.00 + $.15 per page. Paper No. 25192.

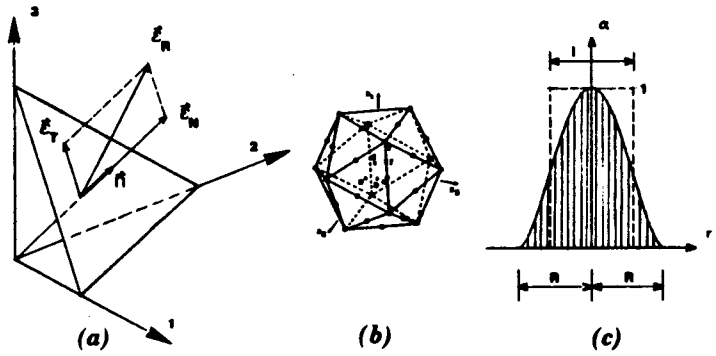

FIG. 1. (a) Strain Components on Microplane; (b) Numerical Integration Points; and (c) Weighting Function for Nonlocal Averaging

$$(\epsilon_R)_i = n_j\epsilon_{ij}; \qquad \epsilon_N = n_i n_j \epsilon_{ij}; \qquad \epsilon_D = n_i n_j \epsilon_{ij} - \epsilon_V \quad \ldots\ldots (1)$$

$$(\epsilon_T)_i = n_k\epsilon_{ik} - n_i(n_j n_k \epsilon_{jk}) = \frac{1}{2}(n_k\delta_{ij} + n_i\delta_{ik} - 2n_i n_j n_k)\epsilon_{jk};$$

$$\epsilon_T = \sqrt{\epsilon_{Ti}\epsilon_{Ti}} \quad \ldots\ldots (2)$$

where Latin lower case subscripts refer to Cartesian coordinates x_i (i = 1, 2, 3); repetition of subscripts implies summation; ϵ_R = the strain vector on a microplane whose unit normal is n_i; ϵ_T and ϵ_T = the tangential vector component of ϵ_R and its magnitude; ϵ_{Ti} = the components of ϵ_T; and ϵ_N = the normal strain component on the microplane [Fig. 1(*a*)]. The normal strain vector is separated into volumetric strain $\epsilon_V = \epsilon_{kk}/3$ and deviatoric strain ϵ_D (i.e., $\epsilon_N = \epsilon_V + \epsilon_D$). This split, proposed by Bažant, makes it possible to obtain any value of elastic Poisson ratio between -1 and 0.5 and, more importantly, has proven essential for allowing good representation of post-peak softening for both tension and compression.

Hypothesis II

Each microplane resists not only normal strain ϵ_N, but also shear strains, ϵ_T, whose vector ϵ_T is assumed to keep the same direction as the vector of shear stresses σ_T. In the initial formulation by Bažant and Oh (1983, 1985), the resistance to ϵ_T was neglected, which sufficed to model multidirectional tensile cracking. However, if compression response should be modeled simultaneously, resistance to ϵ_T must be considered, or else the ratio of compression and tensile strengths would be incorrect and snap-back instability would develop soon after the peak stress in compression.

Hypothesis III

The response on each microplane depends on the mean lateral strain ϵ_L, which is equivalent to the dependence on the volumetric strain $\epsilon_V = \epsilon_{kk}/3$. This feature was necessary for modeling triaxial test data for very high confining pressures, but not for other data.

Hypothesis IV

The stress-strain curves for each microplane are path-independent as long as there is no unloading on the microplane. During each unloading and reloading, which is defined separately on each microplane, the curves of the stress and strain differences from the state at the start of unloading are also path-independent. Thus, all macroscopic path-dependence is produced by various combinations of loading and unloading on all the microplanes. Some microplanes may get unloaded even for macroscopically monotonic or virgin loading, thus making the response path-dependent. The number of possible macroscopic path directions is enormous (for 21 microplanes there are 2^{21} possible tangential stiffness matrices in each loading step, due to all possible combinations of loading and unloading).

Hypothesis V

The volumetric, deviatoric, and shear responses on each microplane are mutually independent. This, of course, greatly simplifies data fitting and suffices to fit each datum.

Microplane Stress-Strain Relations and Damage Rule

In this work we adopt the stress-strain relations of Bažant and Prat (1988), with only some minor simplifications. According to the foregoing hypotheses, the behavior on the microplane level can be described by nontensorial path-independent total stress-strain relations of the form: $\sigma_V = F_V(\epsilon_V)$, $\sigma_D = F_D(\epsilon_D)$, $\sigma_T = F_T(\epsilon_T)$. For two reasons, namely representation of unloading and application of the nonlocal damage concept, it is convenient to cast the total stress-strain relation in the form

$$\sigma_V = C_V\epsilon_V, \qquad \sigma_D = C_D\epsilon_D, \qquad \sigma_T = C_T\epsilon_T \quad \ldots\ldots (3)$$

in which, except for volumetric compression

$$C_V = C_V^0(1 - \omega_V), \qquad C_D = C_D^0(1 - \omega_D), \qquad C_T = C_T^0(1 - \omega_T) \quad \ldots\ldots (4)$$

The last relations are co-opted from continuum damage mechanics, for which application on the microplane level is simpler than for the classical formulations on the macrocontinuum level because all the variables on the microplane are scalar. C_V, C_D, C_T represent the secant moduli, which are variable; $C_V = F_V(\epsilon_V)/\epsilon_V$, $C_D = F_D(\epsilon_D)/\epsilon_D$, $C_T = F_T(\epsilon_T)/\epsilon_T$; C_V^0, C_D^0, and C_T^0 are the initial values of C_V, C_D, and C_T corresponding to elastic behavior; and ω_V, ω_D, and ω_T are volumetric, deviatoric, and shear damage on the microplane level. Fitting of certain test data by Bažant and Prat (1988) led to the following approximation for virgin loading:

$$\text{for } \epsilon_V \geq 0: \qquad \omega_V = 1 - \left(\exp - \left|\frac{\epsilon_V}{e_1}\right|^m\right) \quad \ldots\ldots (5)$$

$$\text{for } \epsilon_D \geq 0: \qquad \omega_D = 1 - \exp\left(-\left|\frac{\epsilon_D}{e_1}\right|^m\right) \quad \ldots\ldots (6a)$$

$$\text{for } \epsilon_D < 0: \qquad \omega_D = 1 - \exp\left(-\left|\frac{\epsilon_D}{e_2}\right|^n\right) \quad \ldots\ldots (6b)$$

$$\omega_T = 1 - \exp\left(-\left|\frac{\epsilon_T}{e_3}\right|^k\right) \quad \ldots\ldots (7)$$

where e_1, e_2, e_3, m, n, and k = empirical material constants. Note that ϵ_T cannot be negative, since it represents a magnitude (description of shear by means of shear-strain magnitude ϵ_T is made possible by hypothesis II). In the volumetric behavior there is no damage ($\omega_V = 0$) and the response for virgin loading is described by

$$\text{for } \epsilon_V < 0: \qquad C_V = C_V^0\left[\left(1 + \left|\frac{\epsilon_V}{a}\right|\right)^{-p} + \left|\frac{\epsilon_V}{b}\right|^q\right] \quad \ldots\ldots (8)$$

where a, b, p, and q = empirical constants.

For the description of unloading and reloading, we introduce a simpler rule than that in Bažant and Prat (1988), assuming that the tangential moduli for unloading or reloading are equal to the initial elastic moduli. This simplification, of course, would not suffice for a good description of large unloading cycles, but it seems adequate to represent the moderate degree of unloading that occurs on some microplanes during postpeak softening.

Virgin loading for ϵ_V occurs when $\epsilon_V \Delta\epsilon_V \geq 0$ and $(\epsilon_V - \epsilon_V^{\max})(\epsilon_V - \epsilon_V^{\min}) \geq 0$, where $\epsilon_V^{\max}$, $\epsilon_V^{\min}$ are the maximum and minimum values of ϵ_V that have occurred so far; otherwise unloading or reloading takes place. The loading criteria for ϵ_D and ϵ_T are analogous. The increment of ϵ_T must for this purpose be defined as $\Delta\epsilon_T = |\epsilon_T + \Delta\epsilon_T| - |\epsilon_T|$, not as $|\Delta\epsilon_T|$ (which is always positive).

Incremental Macroscopic Stress-Strain Relations

For incremental solutions with incremental loading, the total stress-strain relations need to be differentiated to yield incremental relations: $d\sigma_V = C_V d\epsilon_V + \epsilon_V dC_V$, $d\sigma_D = C_D d\epsilon_D + \epsilon_D dC_D$, $d\sigma_T = C_T d\epsilon_T + \epsilon_T dC_T$. For iterative solutions, it is convenient to introduce incremental moduli $\hat{C}_V$, $\hat{C}_D$, and $\hat{C}_T$, which may be chosen but must be equal to or larger than C_V, C_D, and C_T. The foregoing incremental relation may be rewritten in the form

$$\Delta\sigma_V = \hat{C}_V \Delta\epsilon_V - \Delta\sigma_V''; \qquad \Delta\sigma_D = \hat{C}_D \Delta\epsilon_D - \Delta\sigma_D'';$$

$$\Delta\sigma_T = \hat{C}_T \Delta\epsilon_T - \Delta\sigma_T'' \quad \ldots\ldots (9)$$

in which

$$\Delta\sigma_V'' = -\epsilon_V \Delta C_V + (\hat{C}_V - C_V)\Delta\epsilon_V; \qquad \Delta\sigma_D'' = -\epsilon_D \Delta C_D + (\hat{C}_D - C_D)\Delta\epsilon_D;$$

$$\Delta\sigma_T'' = -\epsilon_T \Delta C_T + (\hat{C}_T - C_T)\Delta\epsilon_T \quad \ldots\ldots (10)$$

$\Delta\sigma_V''$, $\Delta\sigma_D''$, and $\Delta\sigma_T''$ are formally treated as inelastic stress increments in a step-by-step iterative solution.

As shown in the previous work, stress equilibrium between the micro- and macrolevels may be approximately enforced by the virtual work equation

$$\frac{4\pi}{3}\Delta\sigma_{ij}\delta\epsilon_{ij} = 2\int_S (\Delta\sigma_N \delta\epsilon_N + \Delta\sigma_{Tr}\delta\epsilon_{Tr})F(\mathbf{n})dS \quad \ldots\ldots (11)$$

where $\mathbf{n}$ = the unit vectors normal to the microplanes; and $\delta\epsilon_{ij}$, $\delta\epsilon_N$, and $\delta\epsilon_{Tr}$ represent the small variations on the macro- and microlevels. The left-hand side of Eq. 11 represents the macroscopic work in a unit sphere of material, while the right-hand side represents the microscopic work over the surface of the same sphere. The factor 2 results from the need of the integral to extend only over a hemisphere surface, S. $F(\mathbf{n})$ is a weight function of

the normal directions $\mathbf{n}$, which can introduce anisotropy of the material in its initial state. We assume $F(\mathbf{n}) = 1$, which implies isotropy. Substituting Eqs. 1, 7, and 9, one can get from Eq. 11 the incremental macroscopic stress-strain relation

$$\Delta\sigma_{ij} = C_{ijkm}\Delta\epsilon_{km} - \Delta\sigma_{ij}'' \quad \ldots\ldots (12)$$

in which

$$C_{ijkm} = \frac{3\pi}{2}\int_S \left[(\hat{C}_D - \hat{C}_T)n_i n_j n_k n_m + \frac{1}{3}(\hat{C}_V - \hat{C}_D)n_i n_j \delta_{km} + \frac{1}{4}\hat{C}_T(n_i n_k \delta_{jm} + n_i n_m \delta_{jk} + n_i n_k \delta_{im} + n_j n_m \delta_{ik})\right]F(\mathbf{n})dS \quad \ldots\ldots (13)$$

$$\Delta\sigma_{ij}'' = \frac{3\pi}{2}\int_S \left[n_i n_j(\Delta\sigma_V'' + \Delta\sigma_D'') + \frac{1}{2}(n_i\delta_{rj} + n_j\delta_{ri} - 2n_i n_j n_r)\Delta\sigma_{Tr}''\right]F(\mathbf{n})dS \quad \ldots\ldots (14)$$

where C_{ijkm} = the macroscopic incremental material stiffness tensor; and $\Delta\sigma_{ij}''$ = the associated macroscopic inelastic stress increments. To make the calculations efficient, the tensorial coefficients in Eqs. 13 and 14, such as $n_i n_j n_k n_m$, $n_j n_k \delta_{im}$, are generated once at the beginning of the analysis and stored in the computer memory.

Tensor C_{ijkm} can have different values depending on the choice of $\hat{C}_V$, $\hat{C}_D$, and $\hat{C}_T$. Following are the two basic choices.

1. One choice is to set $\hat{C}_V = C_V$, $\hat{C}_D = C_D$, $\hat{C}_T = C_T$ for the integration points that are loading, and $\hat{C}_V = C_V^0$, $\hat{C}_D = C_D^0$, $\hat{C}_T = C_T^0$ for those that are unloading or reloading. The resulting tensor C_{ijkm} changes from step to step. It is anisotropic and nonsymmetric, except when $\hat{C}_V = \hat{C}_D$. When there is no unloading, the resulting C_{ijkm} represents the secant stiffness tensor.
2. Another choice is to set $\hat{C}_V = C_V^0$, $\hat{C}_D = C_D^0$, $\hat{C}_T = C_T^0$ for both loading and unloading-reloading. In this case C_{ijkm} is always symmetric and equal to the initial stiffness tensor C_{ijkm}^0, which is here considered to be isotropic; $C_{ijkm}^0 = (K - 2G/3)\delta_{ij}\delta_{km} + G(\delta_{ik}\delta_{jm} + \delta_{im}\delta_{jk})$ where K, G = initial elastic bulk and shear moduli; $K = E/3(1 - 2\nu)$ where E = Young's modulus and ν = Poisson ratio.

Computational efficiency is usually higher for the second choice because of the following advantages: Tensor C_{ijkm}^0 is always the same, so the structural stiffness matrix need not be recalculated at each iteration of each loading step. All the inelastic effects are then represented by $\Delta\sigma_{ij}''$, a tensor of fewer components than C_{ijkm}^0. The iterative procedure in this case coincides with the well-known initial stiffness method (e.g., Owen and Hinton 1980). When we discuss nonlocal generalization we will see another advantage: Tensor C_{ijkm}^0 is always local and symmetric.

The first choice usually increases computational requirements, since C_{ijkm} needs to be recalculated in each loading step. However, the iterative process generally converges faster. In the interest of stability of computations, one should keep the values of C_{ijkm} for all the iterations of the same step the same as in the first iteration, in which the values of C_{ijkm} are determined on the basis of the stresses and strains solved in the previous load step.

There are also instances where it is necessary to calculate tangential stiffness tensor C'_{ijkm} (i.e., the stiffness tensor providing the relation $d\sigma_{ij} = C'_{ijkm} d\epsilon_{km}$). For example, in plane stress analysis (in plane x_1, x_2), the stiffness coefficients C'_{33km} are needed to ensure that the transverse stresses σ_{33} vanish. These coefficients can be calculated as the σ_{33}-values when each variable ϵ_{ij} is 1, while all the others are 0 (and $\Delta\sigma_{ij} = 0$). This procedure is, of course, equivalent to calculating C_{ijkm} from Eq. 12 with $\hat{C}_V = C'_V$, $\hat{C}_D = C'_D$, and $\hat{C}_T = C'_T$, where for virgin loading $C'_V = dF_V/d\epsilon_V$, $C'_D = dF_D/d\epsilon_D$, and $C'_T = dF_T/d\epsilon_T$ (tangential moduli for the microplane), and $\hat{C}_V = C^0_V$, $\hat{C}_D = C^0_D$, and $\hat{C}_T = C^0_T$ for unloading and reloading.

Another case where C'_{ijkm} must be calculated is where the equilibrium response path of the structure is suspected to exhibit bifurcations. Contrary to widespread opinion, stability of iterations does not guarantee that bifurcations are absent or that a stable postbifurcation path is followed. Criteria involving C'_{ijkm} and the lowest eigenvalue of the associated tangential stiffness of the structure need to be checked (Bažant 1988a,b).

Material Parameters and Poisson's Ratio

Matching of Eq. 11 to Hooke's law yields the Young's modulus and Poisson's ratio (Bažant and Prat 1988)

$$E = (1 - 2\nu)C^0_V, \qquad \nu = \frac{5 - 2\eta - 3\xi}{10 + 2\eta + 3\xi}, \qquad \eta = \frac{C^0_D}{C^0_V}, \qquad \xi = \frac{C^0_T}{C^0_V} \quad \ldots\ldots (15)$$

Inverting these relations, one gets

$$\frac{C^0_T}{C^0_V} = \frac{10(1 - 2\nu)}{9(1 + \nu)}\eta \quad \ldots\ldots (16)$$

If $\eta \to 0$ and $\xi \to 0$, then $\nu \to 0.5$; and if $\eta \to \infty$ or $\xi \to \infty$, or both, then $\nu \to -1$. We see that ν satisfies the well-known thermodynamic restriction, namely $-1 < \nu < 0.5$, and that the entire range of ν can be obtained with the present microplane model. (This was not the case for the previous microplane models, in which the idea of splitting ϵ_N into ϵ_V and ϵ_D did not exist.) In the fitting of test data, it is convenient to take the given (measured) values of E (Young's modulus) and ν (Poisson's ratio) as the basic parameters. The value of the ratio $\eta = C^0_D/C^0_V$ may be chosen as any real positive number (so as to optimize the fit of given test data). Then Eq. 15 yields $C^0_V = E/(1 - 2\nu)$, and Eq. 16 provides

$$C^0_T = \frac{1}{3}\left(\frac{5(1 - 2\nu)}{1 + \nu} - 2\eta\right)C^0_V \quad \ldots\ldots (17)$$

Bažant and Prat (1988) found $\eta = 1$ to be a good choice for fitting of all the test data on concretes. The initial Poisson's ratio (ν) and Young's modulus (E) for concrete is known or determined in advance, and parameters a, b, p, q, e_1, e_2, e_3, m, n, and k have to be found by data fitting. Parameters a, b, p, and q can be found independently of the others by fitting hydrostatic pressure test data for compression ($\epsilon_V < 0$). The exponents m, n, and k can be taken as constants. Therefore, only three free parameters (e_1, e_2, and e_3) have to be found by fitting triaxial test data other than the hydrostatic pressure curve. This is not a difficult task (in detail, see Bažant and Prat 1988).

Integration over Hemisphere

The microplane model trades conceptual simplicity for extensive computer time requirements. Thus, numerical efficiency is very important. The integrals in Eqs. 13 and 14 need to be evaluated numerically. This must be done a great number of times—in every load step, in every iteration of the step, and in every integration point of every finite element. Therefore, the evaluation of these integrals over a hemisphere must be as efficient as possible. This problem has been studied in detail. Efficient Gaussian-type formulas for integration over a unit hemisphere have been identified (Stroud 1971), and some new ones, superior in a certain respect, have been found (Bažant and Oh 1985, 1986). These formulas generally approximate the integrals in the form

$$\frac{4\pi}{3}\int_S \simeq 6\sum_{\alpha=1}^{n} w_\alpha F_\alpha \quad \ldots\ldots (18)$$

in which subscrirpt α refers to a certain discrete set of microplanes characterized by the spatial discretization of their normals associated with points on a unit hemisphere, and w_α are the weights (numerical integration coefficients) for these directions. In the present study, Bažant and Oh's (1985, 1986) 21-point integration formula is used [Fig. 1(*b*)]. Any known formula with a lesser number of points does not give sufficient accuracy in the strain-softening regime. When there are symmetries (plane strain, axisymmetry), the number of integration points can, of course, be reduced (e.g., for plane strain or stress, the 21-point formula reduces to a 14-point formula).

Exponential Algorithm for Load Steps

In every iteration of rth load or time step, we can use the known macrostrains $\epsilon_{ij(r)}$ and their known increments $\Delta\epsilon_{ij(r)}$ to calculate the strains and strain increments on each microplane based on the kinematic constraint (Eq. 1). Then we can use the known values of $\epsilon_N = \epsilon_V + \epsilon_D$, ϵ_{Ti}, $\Delta\epsilon_N = \Delta\epsilon_V + \Delta\epsilon_D$, and $\Delta\epsilon_{Ti}$, to calculate the stresses on each microplane by solving the differential equations (Eq. 9). Each of these equations could be solved by using a central difference approximation. However, such an approximation often appears unstable when the stress-strain relation has a negative slope (strain softening), and, even if the computations remain stable, a large error is usually accumulated. The result is that the stress is not reduced exactly to zero at very large strains.

These drawbacks can be eliminated by the so-called exponential algorithm, initially developed for aging creep of concrete (Bažant 1971, Bažant and Wu 1974) as a refinement of the viscoelastic algorithms of Zienkiewicz et al. (1968) and Taylor et al. (1970). Later, Bažant and Chern (1985) extended this algorithm to creep with strain softening. We now adapt this exponential algorithm to the microplane model.

The basic idea of the exponential algorithm is that the integration formula is the exact solution of the differential equation obtained for the current loading step under the assumption that the material properties, the loads, and the prescribed inelastic strain rates are constant in time. To develop the formula of the exponential algorithm for our case, we proceed similarly to Bažant and Chern (1985), using an analogy to Maxwell's spring-dashpot model. The

response in each step is then similar to stress relaxation, and the advantage is that stress relaxation always ultimately yields a zero stress value if the load step is very long. Even though our problem is time-independent, we associate with the load steps a fictitious time t. Then, for each microplane and for both (normal and tangential) directions, it is possible to rewrite the stress-strain relation so that it formally looks like the equation for Maxwell's model. Since the relations for ϵ_V, ϵ_D, and ϵ_T are the same, we now drop subscripts V, D, and T. From $\sigma = C\epsilon$, we have $\dot{\sigma} = C\dot{\epsilon} + \dot{C}\epsilon$, i.e.

$$\dot{\sigma} + \frac{\sigma}{E} = C_a\dot{\epsilon} \quad \text{(19)}$$

where the superior dots denote time derivatives, $E = -C_a/\dot{C}$, $\dot{C} = (dC/d\epsilon)\dot{\epsilon}$, $\dot{\epsilon} = \Delta\epsilon/\Delta t$, and $C_a = (C_r + C_{r+1})/2$ for time-step number r. In every time step $\Delta t_r = t_{r+1} - t_r$. E can be approximated as a constant, and then the exact solution of Eq. 18 is of the form

$$\sigma(t) = Ae^{-(t-t_r)/E} + C_aE\dot{\epsilon} \quad \text{(20)}$$

where A = an integration constant. From the initial condition $\sigma = \sigma_r$ at $t = t_r$, it follows that

$$\sigma(t) = \sigma_r e^{-(t-t_r)/E} + (1 - e^{-(t-t_r)/E})C_aE\Delta\epsilon \quad \text{(21)}$$

For the end of the time step, $t = t_{r+1} = t_r + \Delta t$, we get

$$\sigma_{r+1} = \sigma_r + \Delta\sigma = \sigma_r e^{-\Delta z} + (1 - e^{-\Delta z})C_a\frac{\Delta\epsilon}{\Delta z} \quad \text{(22)}$$

in which $\Delta z = \Delta t/E = -\Delta C/C_a$. Eq. 22 can be rewritten in the form of a pseudo-elastic stress-strain relation for each microplane stress component

$$\Delta\sigma = D\Delta\epsilon - \Delta\sigma'' \quad \text{(23)}$$

where

$$D = C_a\frac{1 - e^{-\Delta z}}{\Delta z} \quad \text{(24)}$$

and $\Delta\sigma'' = (1 - e^{-\Delta z})\sigma_r$ = inelastic stress increment (and $\Delta\epsilon'' = \Delta\delta''/D$ = inelastic strain increment). For overall efficiency, however, it is usually preferable to use the initial elastic modulus C^0 instead of the incremental modulus D, so as to avoid recalculation of the structural stiffness matrix $\mathbf{K}$ for the iterations. In that case, one uses the microplane stress-strain relations $\Delta\sigma = C^0\Delta\epsilon - \Delta\sigma''$, which are made equivalent to Eq. 23 by setting

$$\Delta\sigma'' = (1 - e^{-\Delta z})\sigma_r + (C^0 - D)\Delta\epsilon \quad \text{(25)}$$

where for $\Delta\epsilon$ the value from the preceding iteration or load step may be used.

This algorithm, as well as the similar previous ones, is called exponential because its formula typically involves an exponential function. Attaching subscripts V, D, and T, one may use the foregoing formulas to determine the stress increments on each microplane and in both (normal and tangential) directions. The stress increment on the macrolevel is then determined using

numerical integration over the unit hemisphere (with 21 integration points), as already described. Numerical experience with the present algorithm indicated excellent stability and good accuracy, as checked by time-step refinement.

The present integration scheme also has the advantage that any creep law for concrete can be easily incorporated into the microplane model because numerical integration for the creep law of concrete is similar and entails the same kind of numerical stability problems as it does for strain softening.

Nonlocal Generalization of Microplane Model

Macroscopic behavior of concrete requires a constitutive model that exhibits strain softening (i.e., a decrease of stress at increasing strain), or in general a loss of positive definiteness of the tangential moduli (stiffness) matrix of the material. In concrete, strain softening is due to degradation of material stiffness caused by microcracking. In classical local continuum analysis by the finite element method, strain localization engenders problems of instability, lack of objectivity, and spurious mesh sensitivity (Bažant 1976, 1986; Bažant and Belytschko 1988; Bažant et al. 1984). These problems can be avoided by using a nonlocal continuum.

A nonlocal continuum is a concept in which the stress at a point depends not only on the strain at the same point (local dependence) but also on the strains within a certain neighborhood of the point; in particular, on a certain weighted spatial average of the strains from the neighborhood. This concept, introduced in elasticity by Kröner (1968), Eringen and Edelen (1972), Krumhansl (1968), Levin (1971), and others, has been applied to the strain-softening continuum by Bažant (1984c) and Bažant et al. (1984). However, the early form, called the imbricate continuum, proved too cumbersome.

A more effective form, in which only the variables associated with strain softening are nonlocal and all the other variables, especially the strain as a kinematic variable and the elastic strain, are local, was proposed by Bažant and Pijaudier-Cabot (1987) and Pijaudier-Cabot and Bažant (1987) and further developed in Bažant and Pijaudier-Cabot (1988) and Bažant and Lin (1988a, 1988b). In this formulation, called the nonlocal damage theory, the nonlocal (spatially averaged) quantity is the energy dissipated as a result of strain softening. An important advantage of this formulation is that, in contrast to the classical fully nonlocal continuum theory, the equations of equilibrium and the boundary conditions are of the same form as in the local continuum theory, which is a useful feature for finite element programming. Another advantage over the fully nonlocal continuum is that no zero-energy periodic modes of instability exist.

In the case of the present microplane model, the variables that control strain softening are the damage variables ω_V, ω_D, and ω_T. These variables are calculated from macrostrain ϵ_{ij} by means of the microplane strain components ϵ_V, ϵ_D, and ϵ_T, as indicated in Eqs. 4–7. The nonlocal generalization is achieved merely by replacing ω_V, ω_D, and ω_T in Eqs. 4–7 with nonlocal damage variables $\bar{\omega}_V$, $\bar{\omega}_D$, and $\bar{\omega}_T$, which are calculated from nonlocal macrostrains $\bar{\epsilon}_{ij}$ by means of the resolved microplane components of nonlocal strain, $\bar{\epsilon}_V$, $\bar{\epsilon}_D$, and $\bar{\epsilon}_T$. For the load increments in which unloading or reloading takes place, the local formulation is used; i.e., the strains ϵ_V, ϵ_D,

ϵ_T in the relations $\sigma_V = C_V\epsilon_V$, $\sigma_D = C_D\epsilon_D$, and $\sigma_T = C_T\epsilon_T$ are local, and so is ϵ_{ij} in Eqs. 12–14.

The nonlocal macrostrain $\bar{\epsilon}_{ij}$, which is needed at each integration point of each finite element in each loading step, is calculated from the spatial averaging integral

$$\bar{\epsilon}_{ij}(\mathbf{x}) = \frac{1}{V_r(\mathbf{x})}\int_V \alpha(\mathbf{s}-\mathbf{x})\epsilon_{ij}(\mathbf{s})d\mathbf{x} = \int_V \alpha'(\mathbf{s},\mathbf{x})\epsilon_{ij}(\mathbf{s})d\mathbf{x} \quad \ldots\ldots\ldots\ldots\ldots (26)$$

The superimposed bar denotes the averaging operator; $\mathbf{x}$ and $\mathbf{s}$ = coordinate vectors; $\alpha(\mathbf{x})$ = given empirical weight function; V = volume of the entire structure; and

$$V_r(\mathbf{x}) = \int_V \alpha(\mathbf{s}-\mathbf{x})dV(\mathbf{s}), \qquad \alpha'(\mathbf{s},\mathbf{x}) = \frac{\alpha(\mathbf{s}-\mathbf{x})}{V_r(\mathbf{x})} \quad \ldots\ldots\ldots\ldots\ldots (27)$$

In numerical computation, the spatial averaging integral is approximated by a finite sum over all the integration points (whose number is denoted as N) of all the finite elements of the structure. For convenience of programming, the integration points of all elements are included in the sum, even though for some points the value of $\alpha'(\mathbf{s}-\mathbf{x})$ may be zero. The values of $\alpha'(\mathbf{s}-\mathbf{x})$ are generated in advance and stored as an $N \times N$ square matrix. $V_r(\mathbf{x})$ has approximately the same meaning as the representative volume in the statistical theory of heterogeneous materials (Kröner 1968). When the averaging volume protrudes outside the boundary of the body, the points outside the body must be chopped off and the weights scaled up from α to α' so their sum over the points inside the body equals the original (unchopped) averaging volume. Because of this adjustment, α' depends separately on $\mathbf{x}$ and $\mathbf{s}$, whereas α depends only on the distance $|\mathbf{s}-\mathbf{x}|$. The scaling from α to α' causes the matrix of weights α' to become nonsymmetric.

Although a weight function that is uniform over a certain finite representative volume could be used, it is computationally more efficient (and probably more realistic) to use a smooth, bell-shaped weight function. The existing experimental data on the consequences of nonlocal behavior, such as the size effect, are at present insufficient to decide which shape of function $\alpha(\mathbf{x})$ is more correct, partly because of limited scope of the data, and partly because of their random scatter. The initial studies of Bažant and Pijaudier-Cabot (1987) and Bažant and Lin (1988a, 1988b) used for the weight function α, the Gaussian distribution function. This function extends with nonzero values to infinity, although its values are negligible beyond a certain distance from point $\mathbf{x}$ under consideration. Recently, Bažant proposed for spatial averaging the following bell-shaped function [Fig. 1(*c*)], which vanishes for distances greater than R:

$$\alpha(\mathbf{x}) = \left[1-\left(\frac{\rho}{\rho_1}\right)^2\right]^2 \quad \text{for } \rho < \rho_1; \qquad \alpha = 0 \quad \text{for } \rho \geq \rho_1 \quad \ldots\ldots\ldots\ldots (28)$$

where $\rho = r/kl$, $\rho_1 = R/kl$, $\mathbf{x} = x$ or (x,y) or (x,y,z) for one, two, or three dimensions (1D, 2D, 3D); x,y,z = Cartesian coordinates; and

$$\text{for 1D:} \quad r^2 = x^2, \qquad k = \frac{15}{16} = 0.9375 \quad \ldots\ldots\ldots\ldots\ldots\ldots (29a)$$

$$\text{for 2D:} \quad r^2 = (x^2+y^2), \qquad k = \sqrt{\frac{3}{4}} = 0.9086 \quad \ldots\ldots\ldots\ldots\ldots (29b)$$

$$\text{for 3D:} \quad r^2 = (x^2+y^2+z^2), \qquad k = \left(\frac{105}{192}\right)^{1/3} = 0.8178 \quad \ldots\ldots\ldots (29c)$$

These values of k were determined from the condition that the volume under function $\alpha(\mathbf{x})$ should equal the volume under function $\bar{\alpha}(\mathbf{x})$ that is uniform, $\bar{\alpha}(\mathbf{x}) = 1$, for $r < l/2$, with $\bar{\alpha}(\mathbf{x}) = 0$ for $r \geq l/2$, where l represents the characteristic length of the nonlocal continuum, which gives the size of the representative volume.

The assembled structural stiffness matrices of finite element systems for the nonlocal continuum with local strains are in general nonsymmetric (Bažant and Pijaudier-Cabot 1988) for two reasons: (1) For points close to the boundary, the averaging volume of size R protrudes outside the boundary of the body; and (2) the averaging volume for a point that is loading (or unloading) may include other points that are unloading (or loading). The consequences are that: (1) If point m is loading and point n is unloading, the strain at point n affects the response at point m but the strain at point m does not affect the response at point n (because the response at point n is local and at point m is nonlocal); and (2) if point m is outside and point n inside a boundary layer of thickness R, the influence of strain at n on the response at m is stronger than the influence of strain at m on the response at n (because the size of the averaging volume for point n is smaller than that for point m, due to truncation of the averaging volume that protrudes outside the boundary). For an infinite body in which no point is unloading, the stiffness matrices are symmetric. Compared to the Gaussian distribution function, which is nonzero everywhere in the body, the weight function in Eq. 26 mitigates the incidence of nonsymmetry because the weight function is nonzero only in a limited volume.

The original, fully nonlocal (imbricate) model was giving symmetric stiffness matrices. In fact (Bažant 1984c), the assumption of symmetry in the derivation of the field equation from the virtual work equation inevitably leads to the imbricate model. However, this model is too cumbersome to program and suffers from zero-energy periodic modes of instability that must be artificially suppressed. The nonsymmetry of the tangential stiffness matrix in the present nonlocal formulation was deemed suspect initially, but after considerable numerical experience (e.g., Bažant and Lin 1988a, 1988b) it does not appear to cause problems, probably because the nonsymmetry arises only from damage, a phenomenon for which physics actually imposes no symmetry requirements.

In the present calculations, nonsymmetry of the structural stiffness matrix was avoided altogether by always using the initial elastic stiffness matrix for the iterations. Thus, the symmetry-breaking nonlocal response was incorporated into the inelastic nodal forces.

Numerical Algorithm

1. Before the first load step, evaluate and score the initial elastic structural stiffness matrix $\mathbf{K}$. Also, calculate the integration formula coefficients used in the microplane model and the values of the nonlocal averaging function α', and

store them in the computer memory. Initialize.

2. Loop on load steps.

3. Assign to column matrix $\mathbf{f}^L$ the load values prescribed for the end of the current load step. Impose the boundary conditions of prescribed displacement increments. Initialize unknown $\Delta\mathbf{u} = 0$.

4. Loop on iterations for the same load step.

5. Solve the linear equation system $\mathbf{K}\Delta\mathbf{u} = (\mathbf{f}^L - \mathbf{f})$, where $\Delta\mathbf{u}$ is the column matrix of nodal displacement increments, $\mathbf{K}$ is the initial elastic stiffness matrix, and $\mathbf{f}$ is the column matrix of the resisting nodal forces obtained previously. In the first iteration, Δ denotes the increment corresponding to the sum of the change of the loads prescribed for this step and the unbalanced, initially existing nodal forces, and in subsequent iterations Δ denotes the increment from one iteration to the next at no change of prescribed loads. From $\Delta\mathbf{u}$, calculate (Eqs. 1–2) for all the integration points of all the elements the local strain increments $\Delta\epsilon_{ij}$ and the new strain values $\epsilon_{ij}^N = \epsilon_{ij}^P + \Delta\epsilon_{ij}$, where superscript P denotes the previous (old) values obtained either in the last iteration of the previous load step (for the first iteration) or in the preceding iteration of this step (for the subsequent iterations), while superscript N denotes the new (current) values.

6. For each microplane (at each integration point of each finite element), use the local strains $\Delta\epsilon_{ij}$, ϵ_{ij}^P and the corresponding $\Delta\epsilon_V$, $\Delta\epsilon_D$, and $\Delta\epsilon_T$, ϵ_V^P, ϵ_D^P, and ϵ_T^P to decide whether there is virgin loading, unloading, or reloading. If at least one microplane at a certain point undergoes virgin loading, calculate for that point the nonlocal strains $\bar{\epsilon}_{ij}^P$ and $\bar{\epsilon}_{ij}^N$ by spatial averaging of ϵ_{ij}^P and ϵ_{ij}^N, replacing Eq. 26 by a sum. Then use either $\bar{\epsilon}_{ij}^P$ (for virgin loading) or ϵ_{ij}^P (otherwise) to determine for each microplane (at each integration point of each element) the values of ω_V^P, ω_D^P, ω_T^P, C_V^P, C_D^P, and C_T^P (Eqs. 4–8). Similarly, use either $\bar{\epsilon}_{ij}^N$ (for virgin loading) or ϵ_{ij}^N (otherwise) to calculate for each microplane (at each integration point of each element) the values of ω_V^N, ω_D^N, ω_T^N, C_V^N, C_D^N, and C_T^N (Eqs. 4–8). From these, calculate for each microplane the increments of the secant moduli, $\Delta C_V = C_V^N - C_V^P$, $\Delta C_D = C_D^N - C_D^P$, and $\Delta C_T = C_T^N - C_T^P$, and their averages over the increment, $C_V^a = (C_V^P + C_V^N)/2$, $C_D^a = \ldots$. Then (for the exponential algorithm, Eqs. 22–25) evaluate $\Delta z_V = -\Delta C_V/C_V^a$, $\Delta z_D = \ldots$, $D_V = C_V^a[1 - \exp(-\Delta z_V)]/\Delta z_V$, $D_D = \ldots$ (Eq. 24), and (from Eq. 25) $\Delta\sigma_V'' = [1 - \exp(-\Delta z_V)]\sigma_V^P + (C^0 - D_V)\Delta\epsilon_V$, $\Delta\sigma_D'' = \ldots$ (where $\sigma_V^P = C_V^P\epsilon_V^P$, $\sigma_D^P = \ldots$). As an alternative simpler but less efficient procedure, Eq. 10 can also be used, with $\hat{C}_V = C_V^0, \ldots$; this is not inappropriate for later iterations, for which the change $f^L - f$ becomes small. Note that in this procedure the iterations are treated the same way as a load step with a zero change of load.

7. Now use Eq. 14 to calculate the inelastic macroscopic stress increments $\Delta\sigma_{ij}''$ (for each integration point of each element). Then calculate from $\Delta\sigma_{ij}''$ the column matrix $\Delta\mathbf{f}''$ of inelastic nodal force increments. Finally (noting that $\mathbf{K}\Delta\mathbf{u} = \mathbf{f}^L - \mathbf{f}$), evaluate $\Delta\mathbf{f} = \mathbf{f}^L - \mathbf{f} - \Delta\mathbf{f}''$, which represents the column matrix of the increments of the resisting nodal forces resulting from $\Delta\mathbf{u}$. By adding $\Delta\mathbf{f}$ to $\mathbf{f}$ and $\Delta\mathbf{u}$ to $\mathbf{u}$, update the column matrices of the nodal resisting forces and of the nodal displacements.

8. Calculate the column matrix of residual forces $\mathbf{f}^r = \mathbf{f}^L - \mathbf{f}$. If the ratio $\|\mathbf{f}^r\|/\|\mathbf{f}^L\|$ is less than the prescribed tolerance, terminate calculation of this load step, return to 2 and start the next load step. Otherwise, return to 4 and start the next iteration of the same load step.

Numerical finite element analysis using the present nonlocal formulation exhibited good convergence, excellent stability, and no spurious mesh sensitivity at mesh refinements, even in the strain-softening regime. The rate of convergence of the present nonlocal analysis in the softening range was better than that of a corresponding local formulation obtained by deleting the spatial averaging integrals. Actually, despite the computer time needed to calculate the spatial averages, the overall running time was faster than for the corresponding local finite element code, provided the number of elements was large. This agrees with the experience of Bažant and Lin (1988b) from nonlocal solutions with over 3,000 degrees of freedom. In the case of snapback behavior, the standard measures to achieve stable response may be employed (e.g., controlling the relative displacement of the damage zone, not the load-point displacement).

Numerical Studies and Size Effect

Two examples of finite element analysis using nonlocal microplane models will now be presented. In both, calculations have been made using four-node isoparametric finite elements, with one integration point in example one, and four integration points in example two.

Example One

A concrete specimen with depth-length ratio $d/h = 600/1{,}400$ mm, and thickness $b = 100$ mm is loaded in tension (Fig. 2) in the longitudinal direction. (The thickness choice is arbitrary, because the specimen is analyzed as two-dimensional.) Only one-quarter of the specimen is modeled, and plane strain state is assumed. Strain localization is initiated using weaker elements, as shown by the shaded finite elements in Fig. 2, by decreasing initial modulus of elasticity by 5%. The microplane model parameters for concrete are taken (according to Bažant and Prat 1988) as follows: $a = 0.005$, $b = 0.035$, $p = 1.0$, $q = 1.85$, $e_1 = 0.00006$, $e_2 = 0.0004$, $e_3 = 0.0004$, $m = 1.2$, n

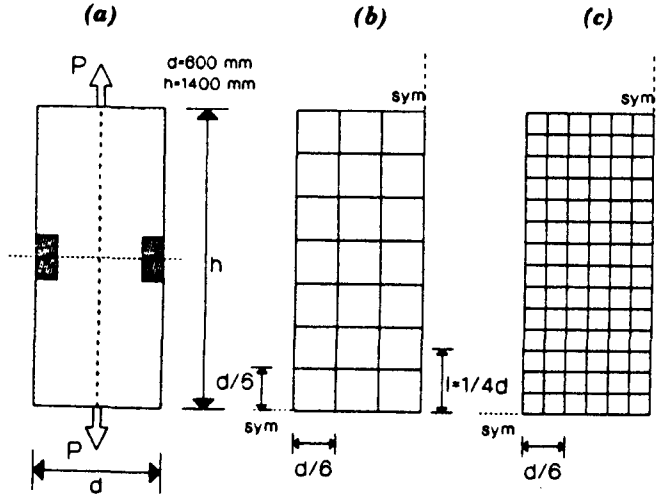

FIG. 2. Rectangular Panel in Example and Finite Element Meshes Used: (*a*) Specimen in Weak Zones; (*b*) Mesh of 21 Elements; and (*c*) Mesh of 24 Elements

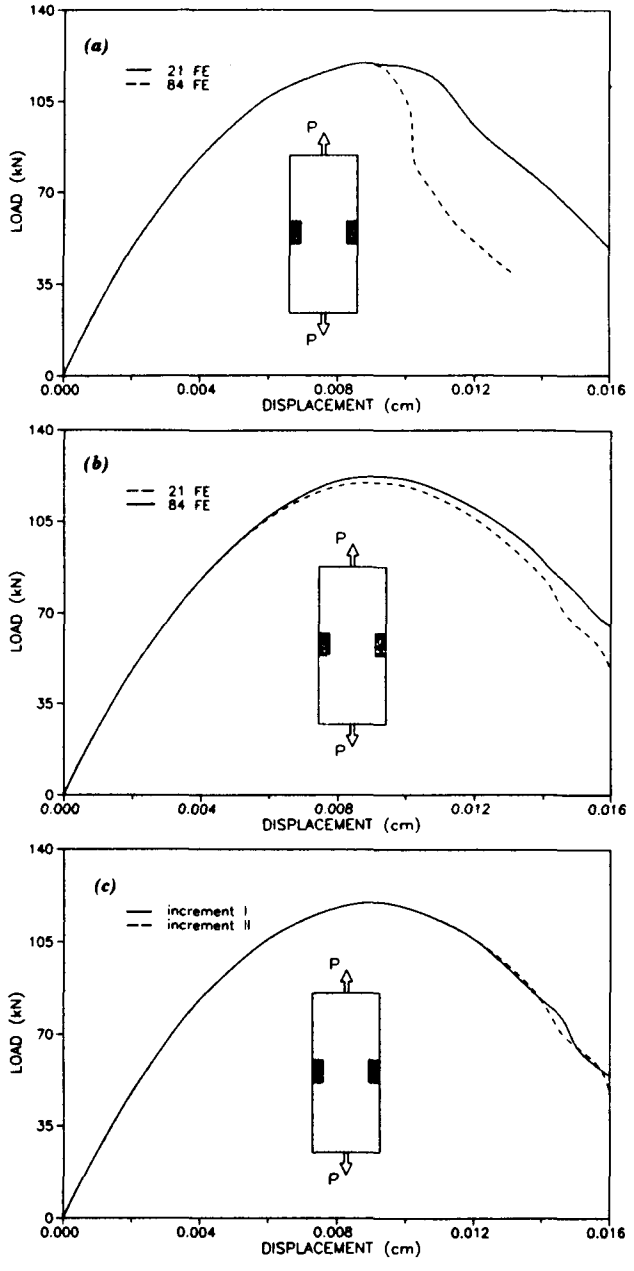

FIG. 3. Load-Displacement Curves of Panel Obtained with Meshes Shown in Fig. 2: (*a*) Local Continuum, Both Meshes; (*b*) Nonlocal Continuum, Both Meshes; and (*c*) Nonlocal Continuum, 21-Element Mesh, Effect of Doubling Prescribed Displacement Increments

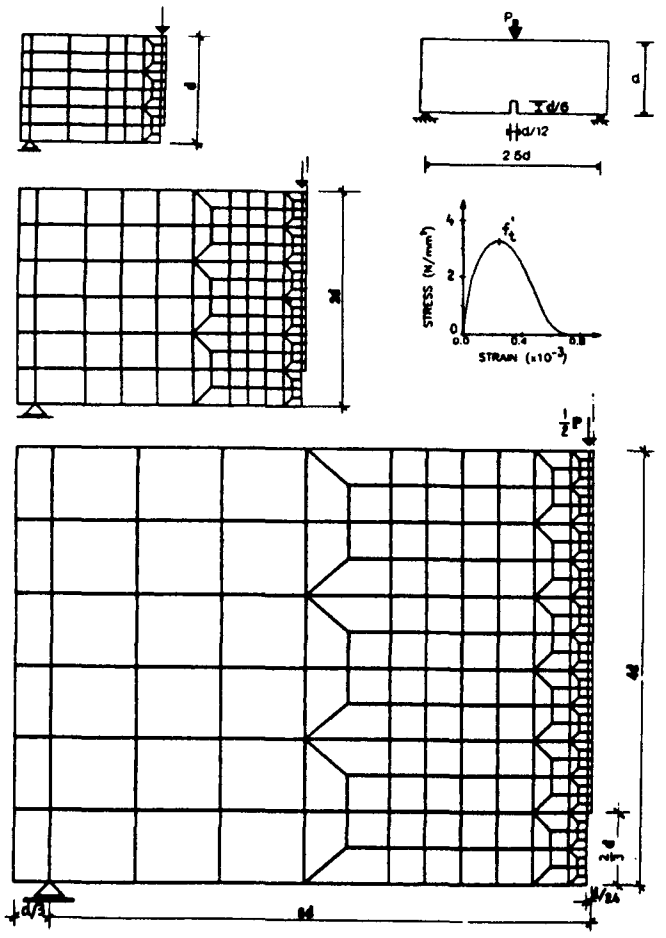

FIG. 4. Three-Point Bend Fracture Specimen, Meshes Used for Its Three Different Sizes, and Uniaxial Stress-Strain Curve

= 1.1, k = 1.1, E_0 = 30,000 N/mm^2, and ν = 0.18. Using these parameters, the uniaxial tensile strength of concrete is calculated as f_t' = 2.05 N/mm^2. In nonlocal analysis, the characteristic length is assumed to be l = 150 mm.

To demonstrate mesh sensitivity in the softening regime, two finite element meshes are generated (Fig. 2), the first with 21 and the second with 84 finite elements. The results of the analysis using local continuum [Fig. 3(*a*)] indicate strong mesh sensitivity. Fig. 3(*b*) shows the results of the analysis using the nonlocal continuum, and there is no mesh sensitivity.

To demonstrate stability of the exponential algorithm, the results for different load steps are plotted in Fig. 3(*c*) (for a mesh of 21 finite elements, nonlocal). For case II the load increment is twice as large as for case I, but the results are still in good agreement.

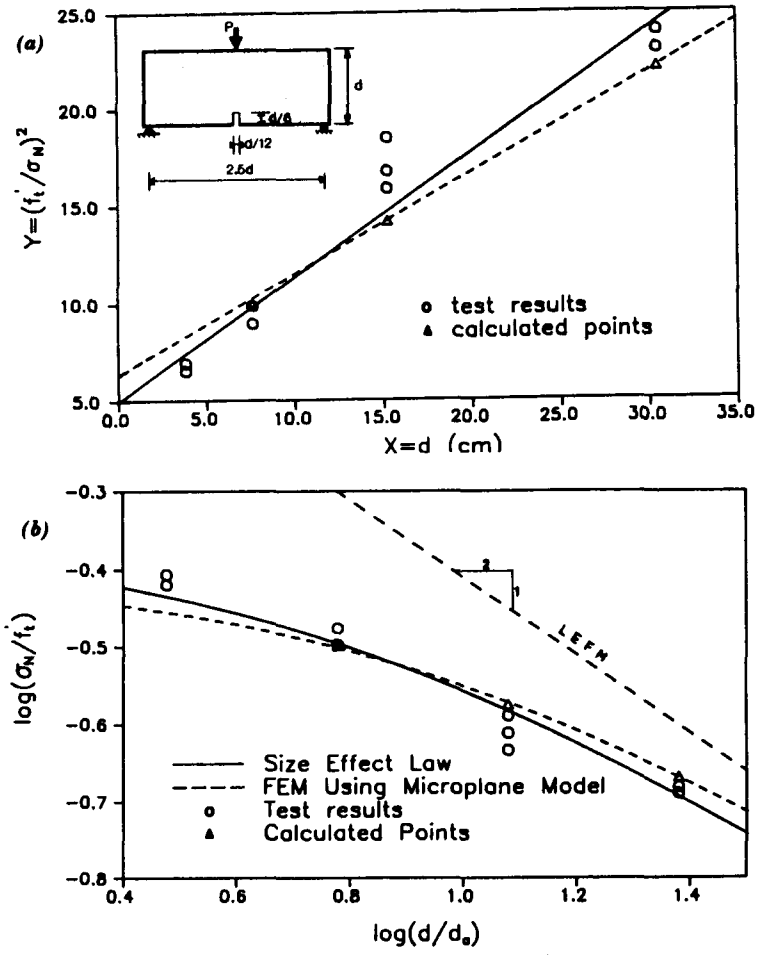

FIG. 5. Nominal Stresses N at Maximum Load Obtained with Meshes in Fig. 4 for Three Specimen Sizes d, Compared with Test Data and Optimum Fit of Data by Size Effect Law: (*a*) Linear Regression Plot

Example 2

To demonstrate that the microplane model using the nonlocal approach correctly describes the fracture of concrete and especially the size effect, three-point-bend specimens are considered. Three specimen sizes of size ratios 1:2:4, with geometrically similar shapes, were used. The finite element meshes and the geometry of the specimens are shown in Fig. 4. The depth of the notch was always one-sixth of the depth of the beam. This type of specimen was tested by Bažant and Pfeiffer (1987) using concrete with a maximum aggregate size d_a = 12.7 mm; the depth of the smallest specimen was d = 7.62 cm. The characteristic length is taken as $l = 3d_a$. The microplane model parameters used in the finite element analysis are partly adjusted by fitting test data for the smallest test specimen, and are as follows:

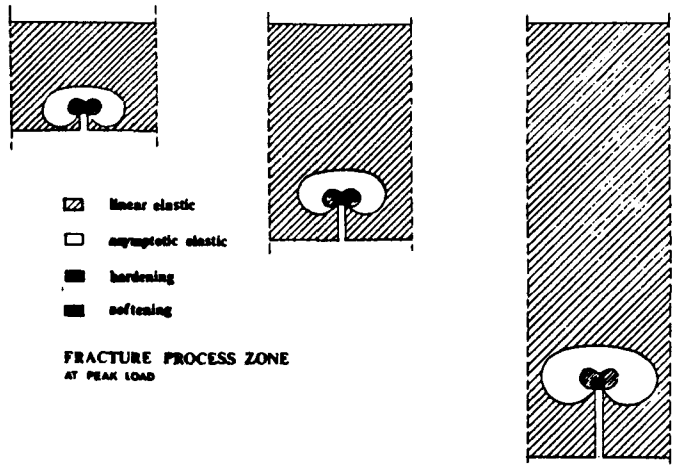

FIG. 6. Fracture Process Zones in Specimens Shown in Fig. 4

a = 0.005, b = 0.035, p = 1.0, q = 1.85, e_1 = 0.000075, e_2 = 0.0012, e_3 = 0.0012, n = 0.5, m = 1.2, k = 1.2, E_0 = 35,000 N/mm^2, and ν = 0.18. From these parameters, the tensile strength of concrete is calculated as f_t' = 3.27 N/mm^2 (Fig. 4).

The maximum loads P, which were previously measured by Bažant and Pfeiffer (1987), are now calculated for each specimen of each size. The values of the nominal stress at failure (σ_N) are calculated as $\sigma_N = P/bd$, where b = specimen thickness (38.1 mm) and d = depth of the specimen. The previous experimental results and the present results of numerical analysis are shown in Figs. 5(*a–b*). The solid and dashed curves represent the optimum fit of the test results with the present model and the fits by the size effect law proposed by Bažant (1984a)

$$\sigma_N = Bf_t'(1 + \beta)^{-1/2}, \qquad \beta = \frac{d}{d_0} \qquad (30)$$

The optimum values for parameters B and d_0 are obtained by linear regression. For the previous test results, these parameters are: B = 0.448 and d_0 = 12.04 mm [Fig. 5(*a*)]. Figs. 5(*a* and *b*) demonstrate a good agreement between the test results and the calculated results.

In addition, Fig. 6 shows the contours of the fracture process zone at peak load for all specimens, calculated from the finite element results. The radius of the fracture process zone is roughly equal to the characteristic length l, increasing slightly as the specimen size increases. The figure also shows the contours of the hardening nonlinear zone around the fracture process zone and of the zone in which the stresses as a function of strains are elastic with an error of less than 5% of f_t'.

Conclusions

1. As confirmed numerically, nonlocal generalization of the microplane model: (1) Is free of spurious mesh sensitivity and localization instabilities; (2) can be

implemented in a finite element code; (3) allows an efficient solution procedure; and (4) can handle both fracture (or damage localization) and nonlinear triaxial behavior with or without strain softening.

2. The nonsymmetry of the tangential stiffness matrix, arising from both the microplane formulation and the nonlocality, seems to pose no computational problems if the load-step algorithm is based on the initial elastic stiffness matrix.

3. The idea of exponential algorithm, in which the load-step stress-strain relation is derived from a certain exact solution of the differential equations of the microplane model, appears to increase computational efficiency. Although the computer work per step becomes larger, the exponential algorithm makes it possible to take much larger loading steps. It also guarantees that stress at the tail of strain-softening behavior gets reduced exactly to zero, regardless of previous numerical errors.

4. The microplane model, which has already allowed an excellent description of the existing test data on nonlinear triaxial behavior as well as unidirectional and multidirectional smeared cracking, is capable of modeling at the same time the tensile fracture.

5. The model is free of spurious mesh sensitivity and exhibits the correct transitional size effect, which was previously experimentally verified for concrete specimens or structures and was approximately described by the size effect law proposed by Bažant (1984).

6. According to the present model, the shape and width of the fracture process zone in concrete varies, albeit mildly, with the specimen size.

7. The method of nonlocal generalization, the exponential algorithm, and the capability to describe fracture with the transitional size effect is not limited to concrete but should be applicable to brittle-plastic materials in general (e.g., ceramic composites, rocks, and stiff soils).

Acknowledgments

Financial support under AFOSR contract No. F49620-87-C-0050DEF with Northwestern University is gratefully acknowledged. Further funds for the numerical algorithm studies were obtained under National Science Foundation grant MSM-8700830. Thanks are due to T. Hasegawa of the Shimizu Institute of Technology, Tokyo, Japan, for some valuable discussions. Partial funding for the material modeling was also obtained from the NSF Science and Technology Center on Advanced Cement-Based Materials at Northwestern University.

Appendix. References

Bažant, Z. P. (1971). "Numerically stable algorithm with increasing time steps for integral-type aging creep." *Proc. First Int. Conf. on Struct. Mech. in Reactor Tech.*, West Berlin, W. Germany, T. A. Jaeger, ed., 4, Part H, 119–126.

Bažant, Z. P., and Wu, S. T. (1974). "Rate-type creep law of aging concrete based on Maxwell Chain." *Matls. and Structs.*, RILEM, Paris, France, 7(37), 45–60.

Bažant, Z. P., and Bhat, P. D. (1976). "Endochronic theory of inelasticity and failure of concrete." *J. Engrg. Mech.*, ASCE, 102(4), 701–722.

Bažant, Z. P. (1976). "Instability, ductility, and size effect in strain-softening concrete." *J. Engrg. Mech.*, ASCE, 102(2), 331–334.

Bažant, Z. P., and Kim, S. S. (1979). "Plastic-fracturing theory for concrete." *J. Engrg. Mech.*, ASCE, 105(3), 407–428.

Bažant, Z. P., and Oh, B. H. (1983). "Crack band theory for fracture of concrete." *Matls. and Structs.*, RILEM, Paris, France, 16(93), 155–177.

Bažant, Z. P. (1984a). "Size effect in blunt fracture: Concrete, rock, metal." *J. Engrg. Mech.*, ASCE, 110(4), 518–535.

Bažant, Z. P. (1984b). "Microplane model for strain-controlled inelastic behavior." *Mechanics of Engineering Materials*, C. S. Desai and R. H. Gallagher, eds., John Wiley and Sons, New York, N.Y., 45–59.

Bažant, Z. P. (1984c). "Imbricate continuum and its variational derivation." *J. Engrg. Mech.*, ASCE, 110(12), 1693–1712.

Bažant, Z. P., and Gambarova, P. G. (1984). "Crack shear in concrete: Crack band microplane model." *J. Struct. Engrg.*, ASCE, 110(9), 2015–2035.

Bažant, Z. P., Belytschko, T. B., and Chang, T. P. (1984). "Continuum model for strain-softening." *J. Engrg. Mech.*, ASCE, 110(12), 1666–1692.

Bažant, Z. P. (1986). "Mechanics of distributed cracking." *Appl. Mech. Rev.*, 39(5), 675–705.

Bažant, Z. P., and Oh, B. H. (1985). "Microplane model for progressive fracture of concrete and rock." *J. Engrg. Mech.*, ASCE, 111(4), 559–582.

Bažant, Z. P., and Chern, J. C. (1985). "Strain-softening with creep and exponential algorithm." *J. Engrg. Mech.*, ASCE, 111(3), 381–390.

Bažant, Z. P., and Oh, B. H. (1986). "Efficient numerical integration on the surface of a sphere." *Zeitschrift für Angewandte Mathematik und Mechanik (ZAMM)*, 66(1), 37–49.

Bažant, Z. P., and Pfeiffer, P. A. (1987). "Determination of fracture energy from size effect and brittleness number." *ACI Matls. J.*, 84(Nov.), 463–480.

Bažant, Z. P., and Pijaudier-Cabot, G. (1987). "Modeling of distributed damage by nonlocal continuum with local strain." *Preprints, Fourth Int. Conf. on Numerical Methods in Fracture Mech.*, San Antonio, Tex., Mar., Pineridge Press, Swansea, United Kingdom, A. R. Luxmore et al., eds., 411–432.

Bažant, Z. P., and Lin, F.-B. (1988a). "Nonlocal smeared cracking model for concrete fracture." *J. Struct. Engrg.*, 114(11), 2493–2510.

Bažant, Z. P., and Lin, F.-B. (1988b). "Nonlocal yield-limit degradation." *Int. J. Num. Methods Engrg.*, 26, 1805–1823.

Bažant, Z. P., and Pijaudier-Cabot, G. (1988). "Nonlocal continuum damage, localization instability and convergence." *ASME J. Appl. Mech.*, 55, 287–293.

Bažant, Z. P., and Prat, P. C. (1988). "Microplane model for brittle plastic material: I. Theory, II. Verification." *J. Engrg. Mech.*, ASCE, 114, 1672–1702.

Bažant, Z. P. (1988a). "Stable states and paths of structures with plasticity or damage." *J. Engrg. Mech.*, ASCE, 114(12), 2013–2034.

Bažant, Z. P. (1988b). "Stable states and stable paths of propagation of damage zones and interactive fractures in cracking and damage." *Proc., France-US Workshop*, ENS, Cachan, France, Sep., J. Mazars and Z. P. Bažant, eds., Elsevier, London, United Kingdom, 183–206.

Bažant, Z. P., and Belytschko, T. (1988). "Strain-softening continuum damage: Localization and size effect," *Proc. Second Int. Conf. on Constitutive Laws of Engrg. Matls.: Theory and Applications*, Tucson, Ariz., Jan., C. S. Desai et al., eds., Elsevier, New York, N.Y., 11–33.

Cedolin, L., dei Poli, S., and Iori, I. (1983). "Experimental determination of the fracture process zone in concrete." *Cement and Concr. Res.* 13, 557–567.

Chen, A. C. T., and Chen, W. F. (1975). "Constitutive relations for concrete." *J. Engrg. Mech.*, ASCE, 101(4), 465–481.

Dougill, J. W. (1976). "Unstable progressively fracturing solids." *J. Appl. Math. and Physics (ZAMP)*, 27, 423–436.

Eringen, A. C., and Edelen, D. G. D. (1972). "On nonlocal elasticity." *Int. J. Engrg. Sci.*, 10, 233–248.4.

Gerstle, K. H., et al. (1980). "Behavior of concrete under multi-axial stress states." *J. Engrg. Mech.*, ASCE, 106(6), 1383–1403.

Gerstle, K. H. (1981). "Simple formulation of biaxial concrete behavior." *ACI J.* 78(1), 62–68.

Kröner, E. (1968). "Interrelations between various branches of continuum mechan-

ics." *Mechanics of Generalized Continua*, E. Klörner, ed., Springer, W. Berlin, W. Germany, 330–340.
Krumhansl, J. A. (1968). "Some considerations of the relations between solid state physics and generalized continuum mechanics." *Mechanics of Generalized Continua*, E. Kröner, eds., Springer, W. Berlin, W. Germany, 298–331.
Levin, V. M. (1971). "The relation between mathematical expectation of stress and strain tensors in elastic microheterogenous media." *Prikl. Mat. Mekh.*, 35, 694–901 (in Russian).
Lin, F. P., et al. (1987). "Concrete model with normality and sequential identification." *Computer and Struct.*, 26(6), 1011–1026.
Ortiz, M. A. (1985). "A constitutive theory for the inelastic behavior of concrete." *Mech. and Matls.*, 4, 67–93.
Pande, G. H., and Xiong, W. (1982). "An improved multi-laminate model of jointed rock masses." *Proc. First Int. Symp. Numerical Models in Geomech.*, Balkema, Rotterdam, the Netherlands, 218–226.
Pijaudier-Cabot, G., and Bažant, Z. P. (1987). "Nonlocal damage theory." *J. Engrg. Mech.*, ASCE, 113, 1512–1533.
Stroud, A. H. (1971). *Approximate calculation of multiple integrals*. Prentice-Hall, Englewood Cliffs, N.J., 296–302.
Taylor, G. I. (1938). "Plastic strain in metals." *J. Inst. Metals*, 62, 307–324.
Taylor, R. L., Pister, K. S., and Goudreau, G. L. (1970). "Thermo-mechanical analysis of visco-elastic solids." *Int. J. Num. Methods Engrg.*, 2, 45–60.
Willam, K. J., and Warnke, E. P. (1974). "Constitutive model for the triaxial behavior of concrete." *Seminar on Concrete Structures Subjected to Triaxial Stresses, Int. Assoc. of Bridge and Struct. Engrg. Conf.*, Bergamo, Italy, May.
Zienkiewicz, O. C., Watson, M., and King, I. P. (1968). "A numerical method of visco-elastic stress analysis." *Int. J. Mech. Sci.* 10, 807–827.
Zienkiewicz, O. C., and Pande, G. N. (1977). "Time-dependent multi-laminate model of rocks—A numerical study of deformation and failure of rock masses." *Int. J. Num. Analytical Meth. Geomech.*, 1, 219–247.